International Journal of Mechanical Sciences 284 (2024) 109766



Contents lists available at ScienceDirect

International Journal of Mechanical Sciences

journal homepage: www.elsevier.com/locate/ijmecsci





Physics-informed deep learning for structural dynamics under moving load

Ruihua Liang [a,b], Weifeng Liu [a], Yuguang Fu [b,*], Meng Ma [a]

[a] Key Laboratory of Urban Underground Engineering of Ministry of Education, Beijing Jiaotong University, Beijing 100044, China
[b] School of Civil and Environmental Engineering, Nanyang Technological University, Singapore 639798, Singapore

ARTICLE INFO

Keywords:
Structural dynamics
Deep learning
Parameter identification
Physics-informed neural network (PINN)
Moving load
Frequency domain

ABSTRACT

Physics-informed deep learning has emerged as a promising approach that incorporates physical constraints into the model, reduces the amount of data required, and demonstrates robustness and potential in dealing with limited datasets for a variety of studies. However, several key challenges still exist, with one being the spectral bias problem of deep learning in the simulation of functions with multi-frequency features. To overcome the challenge, this study proposes a novel physics-informed deep learning method, which integrates physics-informed neural network with Fourier transform so as to solve partial differential equations in the frequency domain, thus alleviating the problem of spectral bias of neural networks in the simulation of multi-frequency functions. In addition, the proposed method is used to focus on the forward simulation and parameter inverse identification issues in structural dynamics under moving loads. To illustrate the superiority of the method, the issues of dynamic response of simply supported beams under moving loads are presented as case studies, and the performance of the method in multiple cases is analysed and discussed. The research results demonstrate the feasibility and effectiveness of the method for structural dynamics simulation and parameter inverse identifications using limited datasets.

1. Introduction

The forward simulation of structural mechanical behavior and the inverse identification of their parameters are significant research areas with applications in mechanical fields, including civil infrastructures [1], soils [2], and mechanical systems [3]. Over the past decades, numerous scientific numerical computational methods and their derivatives have been proposed. These methods solve partial differential equations (PDEs) that describe structural mechanical behavior [4], enabling both forward simulation of structures and inverse identification of structural parameters [5]. The most widely used methods include the finite element method [6], the finite difference method [7], the discrete element method [8], the spectral element method [9], the finite volume method [10], the meshless method [11], and the discontinuous deformation analysis method [12].

In recent years, deep learning research has flourished, demonstrating strong potential in the simulation of structural mechanical behavior [13]. Specifically, deep learning, grounded in mathematical optimization and statistics, enables the construction of models with complex functions and numerous parameters [14]. These models are trained and optimized using vast amounts of data, thereby achieving accurate simulations of structural mechanical behavior [15]. This data-driven approach has shown excellent performance in mechanical behavior simulation [16], structural health monitoring [17,18], load identification [19,20], source localization [21], uncertainty analysis [22], and other research tasks [23,24]. However, in many real-world engineering scenarios, data acquisition for physical systems is often highly complex and costly [25]. This is a significant drawback of deep learning methods, which rely heavily on data, and it poses challenges to their feasibility and reliability in practical applications [26].

To mitigate the data-dependency issue in deep learning, embedded physical information has been introduced, incorporating physical constraints into the optimization of model parameters [27]. Models developed based on these concepts are known as physics-informed neural networks (PINNs) [28]. Due to these physical information-based constraints, PINNs can address forward and inverse problems involving nonlinear physical systems with small datasets or even without labeled data. This method has demonstrated excellent performance and promising potential in various research areas [29], such as simulation of heat transfer problems [30,31], fluid flows [32,33], seismic wavefield [34,35], solid mechanics [36,37], etc. However, existing studies have shown that neural networks struggle to simulate functions with

* Corresponding author.
E-mail address: yuguang.fu@ntu.edu.sg (Y. Fu).

https://doi.org/10.1016/j.ijmecsci.2024.109766
Received 23 June 2024; Received in revised form 29 September 2024; Accepted 29 September 2024
Available online 2 October 2024
0020-7403/© 2024 Elsevier Ltd. All rights are reserved, including those for text and data mining, AI training, and similar technologies.

multi-frequency features [38], common in structural dynamics, a phenomenon known as spectral bias [39]. Multi-frequency features are prevalent in structural mechanical behavior, particularly in structural dynamics, where the structural response under dynamic loading typically exhibits both the modal properties of the structure and the spectral properties of the loading [40]. Moreover, structural dynamics has numerous real-world engineering applications [41], including identifying the dynamic response and structural health of bridges [42], tunnels [43], and other infrastructure [44]. However, traditional PINNs often encounter spectral bias when solving these structural dynamics problems, hindering the use of interpretable AI techniques that incorporate physical information in mechanics and engineering [45]. Therefore, research on mitigating the spectral bias in neural networks is necessary to support further engineering applications of deep learning methods in tasks like structural mechanical behavior simulation and parameter identification [46].

In recent years, several studies have been conducted to mitigate the impact of spectral bias in neural network-based solutions. For example, Chai et al. [47] proposed strategies such as multiscale Fourier feature mapping and revised neuron splitting to solve the spectral bias of the neural network in high-frequency wavefield predictions. Zhao et al. [48] proposed an adaptive method to control spectral bias by regulating spectral norms across convolutional layers through guided gradient flow, thereby reducing overfitting and improving model performance on denoising and inpainting tasks. Ding et al. [49] utilized the modal information of the target system obtained from the numerical analysis, thus realized an accurate neural network solution for the dynamical system based on the modal superposition method. Waheed et al. [50] introduced Kronecker neural networks with adaptive activation functions to overcome the spectral bias in neural networks for wavefield modeling. Existing studies on addressing spectral bias are typically tailored to specific equations or problems, and most of these approaches require the incorporation of labeled data into the construction of the loss function during the solution process. Furthermore, in some researches, the integration of additional techniques makes it challenging for PINN to simultaneously handle both forward and inverse computations [51].

In the solution of differential equations, integral transform methods [52], such as the Fourier transform [53], provide an efficient approach by converting the original equation into a domain that is more amenable to solution [54]. As a general differential equation processing technique, the Fourier transform can be used to effectively circumvent the multi-frequency characteristics present in solutions to structural dynamics problems [55], enabling accurate solutions without relying on labeled data [56]. The aim of this paper is to propose a novel PINN model to mitigate the spectral bias of neural networks and to apply it in solving forward and inverse problems in structural dynamics, thus providing support for their broader application in the future. Specifically, frequency domain physics-informed neural networks (FD-PINN) method is proposed to address the spectral bias of neural networks. This method uses the Fourier transform to convert the original equations into the frequency domain, thereby reducing the difficulty of neural network simulations and improving accuracy. Several case studies involving the dynamic response analysis of a simply supported beam structure under moving loads is conducted to thoroughly analyze and discuss the forward and inverse simulation performances of the FD-PINN models.

The rest of the paper is organized as follows: Section 2 provides a detailed description of the mathematical representation of the structural dynamics problem and the establishment and calculation of the PINN in both the time and frequency domains. Section 3 presents the computational results of the PINN model for forward simulation of structural dynamics in both domains, with an analysis and discussion of the results. Section 4 illustrates the performance of the PINN models in the inverse identification of structural dynamics parameters, including a discussion of the results. Finally, Section 5 concludes the research and presents an outlook for future work.

2. Methodology

In this section, the concept of structural dynamics under moving loads is described in Section 2.1, which provides the preliminary conditions for the subsequent work. Section 2.2 presents the concept of PINN in addressing forward and inverse problems, including a description of the model structure, embedded physical constraints, and the training procedure. Additionally, Section 2.3 details the proposed FD-PINN, covering its solution concept, specific governing equations, implementation procedure, and more.

2.1. Theory of structural dynamics under moving load

The motion of a simply supported Euler-Bernoulli beam under a moving load p with velocity v is studied, and the PDE of motion is given by [57]:

$$EI\frac{\partial^4 u(x,t)}{\partial x^4}+c\frac{\partial u(x,t)}{\partial t}+m\frac{\partial^2 u(x,t)}{\partial t^2}=p\delta(x-vt), \tag{1}$$

where E is Young's modulus; I is the moment of inertia of the cross-section; $u(x, t)$ is the transverse deflection of the beam; c is the damping coefficient; m is the mass per unit length; δ is the Dirac delta function; x is the distance from one support in the direction of motion; t is time; L is the length of the beam.

For a beam with simple supports, the boundary conditions and initial conditions are as follows,

$$u(0,t)=u(L,t)=\frac{\partial^2 u}{\partial x^2}(0,t)=\frac{\partial^2 u}{\partial x^2}(L,t)=0, \tag{2}$$

$$u(x,0)=\frac{\partial^2 u}{\partial t^2}(x,0)=0. \tag{3}$$

The use of the separation of variables method to solve the above PDE is a classical analytical method [58], which assumes the beam displacement solution in the following form [59]:

$$u(x,t)=\sum_{n=1}^{\infty}\phi_n(x)q_n(t), \tag{4}$$

where $\phi_n(x)$ is the nth vibration mode of the beam that satisfies the boundary conditions, and $q_n(t)$ is the generalized coordinate corresponding to the nth mode, it describes the intensity or participation level of the system in the nth mode.

2.2. Physics-informed neural network

PINN is a deep learning framework that integrates physical information and data, which allows approximating the solution of partial differential equations using various neural network models. The PDE to be solved in PINN can be expressed in the following form [45],

$$\mathscr{N}[\mathbf{u}](\mathbf{x})=\boldsymbol{f}(\mathbf{x}),\quad \mathbf{x}\in\Omega, \tag{5}$$

$$\mathscr{B}[\mathbf{u}](\mathbf{x})=\boldsymbol{g}(\mathbf{x}),\quad \mathbf{x}\in\partial\Omega, \tag{6}$$

where $\mathscr{N}[\cdot]$ is a differential operator; $\mathscr{B}[\cdot]$ are the boundary conditions; $\boldsymbol{u}$ is the unknown quantity in the equations, which is the deflection of beams in this study; $\boldsymbol{x}$ is the independent variable in the equation, which is the spatial and time variables in this study; Ω is the calculation domain; $\partial\Omega$ is the boundary of the computational domain; $\boldsymbol{f}(\mathbf{x})$ and $\boldsymbol{g}(\mathbf{x})$ are specific functions regarding the governing equations and boundary conditions, respectively.

The effect of physical information on the PINN is mainly manifested in the loss function, and by optimizing the trainable parameters in the neural network to minimize the loss function, the neural network can approximate the solution of the PDEs. The loss function of PINN in

solving the forward problem can usually be expressed as follows [60,61]:

$$\mathscr{L}(\boldsymbol{\theta}) = w_{\mathrm{DE}}\mathscr{L}_{\mathrm{DE}}(\boldsymbol{\theta}) + w_{\mathrm{BC}}\mathscr{L}_{\mathrm{BC}}(\boldsymbol{\theta}), \tag{7}$$

$$\mathscr{L}_{\mathrm{DE}}(\boldsymbol{\theta}) = \frac{1}{N_{\mathrm{r}}}\sum_{i=1}^{N_{\mathrm{r}}}\left|\mathscr{N}[\mathbf{u}](\mathbf{x}_{\mathrm{r}}^{i}) - \boldsymbol{f}(\mathbf{x}_{\mathrm{r}}^{i})\right|^{2}, \tag{8}$$

$$\mathscr{L}_{BC}(\boldsymbol{\theta}) = \frac{1}{N_{\mathrm{b}}}\sum_{i=1}^{N_{\mathrm{b}}}\left|\mathscr{B}[\mathbf{u}](\mathbf{x}_{\mathrm{b}}^{i}) - \boldsymbol{g}(\mathbf{x}_{\mathrm{b}}^{i})\right|^{2}, \tag{9}$$

where $\boldsymbol{\theta}$ is the trainable parameter vector; $\mathscr{L}_{\mathrm{DE}}(\boldsymbol{\theta})$ and $\mathscr{L}_{\mathrm{BC}}(\boldsymbol{\theta})$ are the loss functions for the governing equations and boundary conditions respectively; $\mathbf{x}_{\mathrm{r}}$ and $\mathbf{x}_{\mathrm{b}}$ are the training data randomly sampled in the respective computational domains; N_{r} and N_{b} are the number of training data. The parameters $\{w_{\mathrm{DE}}, w_{\mathrm{BC}}\}$ are the coefficients for each sub-term in the loss function, which need to be specified in advance.

The network structure for the forward solving of the beam response using PINN is depicted in Fig. 1 (a), and the mechanical information in Eq. (1) is used to form the loss function, where the differentiation calculations can be implemented by the automatic differentiation algorithm in PINN [62].

For inverse problems such as inverse identification of PDE parameters using measured data, the parameters to be identified can be considered as trainable parameters in PINN and the difference between the model output and the measured data can be used to form a loss function. The network structure of PINN in solving the inverse problem is shown in Fig. 1 (b), and the loss function can be represented as:

$$\mathscr{L}(\boldsymbol{\theta}) = w_{\mathrm{DE}}\mathscr{L}_{\mathrm{DE}}(\boldsymbol{\theta}) + w_{\mathrm{BC}}\mathscr{L}_{\mathrm{BC}}(\boldsymbol{\theta}) + w_{\mathrm{ME}}\mathscr{L}_{\mathrm{ME}}(\boldsymbol{\theta}), \tag{10}$$

$$\mathscr{L}_{\mathrm{ME}}(\boldsymbol{\theta}) = \frac{1}{N_{\mathrm{m}}}\sum_{i=1}^{N_{\mathrm{m}}}\left|\mathbf{u}_{\mathrm{acutal}} - \mathbf{u}_{\mathrm{output}}\right|^{2}, \tag{11}$$

where $\mathscr{L}_{\mathrm{ME}}(\boldsymbol{\theta})$is the loss functions for the measurement data; $\mathbf{u}_{\mathrm{acutal}}$ is the actual measurement result; $\mathbf{u}_{\mathrm{output}}$ is the model output result; N_{m} is the number of measurement data, and the parameter w_{ME} is the corresponding coefficient in the loss function.

In addition, recent years have seen the development of various PINN variants, such as Gradient-enhanced physics-informed neural network (gPINN) [63], which incorporates the derivatives of the PDE into the constraints when the network is updated, and Self-adaptive physics-informed neural network (SA-PINN) [64], which facilitates adaptive updates of coefficients in the loss function during model training. These networks empower the solution of PDE equations without the need for labeled data.

2.3. Frequency domain physics-informed neural network

Structural dynamics problems often involve multi-frequency features [65], traditional neural networks might struggle to accurately simulate them. To enhance the capability of PINNs in addressing structural dynamics issues, this paper introduces the FD-PINN method. Specifically, the Fourier transform is employed to convert the original time-domain PDE into the frequency domain, where the frequency components of the solution become simpler. Subsequently, the response spectrum obtained by solving the PINN in the frequency domain is inverse Fourier transformed back to the time domain, thereby obtaining the solution to the original PDE. The network structures of FD-PINN in solving the forward and inverse problem are shown in Fig. 1 (c) and (d).

In the case of the dynamic response of beams under moving loads studied in this paper, the formulation of Eq. (1) in the frequency domain is obtained using the Fourier transform as shown below [66]:

$$EI\frac{\partial^4\hat{u}(x,\omega)}{\partial x^4} + ic\omega\hat{u}(x,\omega) - m\omega^2\hat{u}(x,\omega) = \int_0^{L/v} p\delta(x-vt)e^{-\mathrm{i}\omega t}dt = \frac{p}{v}\mathrm{e}^{\frac{-\mathrm{i}x\omega}{v}}, \tag{12}$$

$$\hat{u}(x,\omega) = \int_0^{L/v} u(x,t)e^{-\mathrm{i}\omega t}dt, \tag{13}$$

where $\hat{u}(x,\omega)$ represents the spectrum of beam displacements, which is the result of $u(x, t)$ in the frequency domain obtained using the Fourier transform; ω is the angular frequency. In addition, when solving the above equation using PINN, an immediate problem is that the neural network is unable to deal with complex numbers. Therefore, the solution of the PDE in the frequency domain is represented in the following form:

$$\hat{u}(x,\omega) = \hat{u}_{\mathrm{r}}(x,\omega) + i\hat{u}_{\mathrm{i}}(x,\omega), \tag{14}$$

substituting this Eq. (14) into Eq. (12) gives the real and complex parts of the equation, respectively, which can be expressed in the following form:

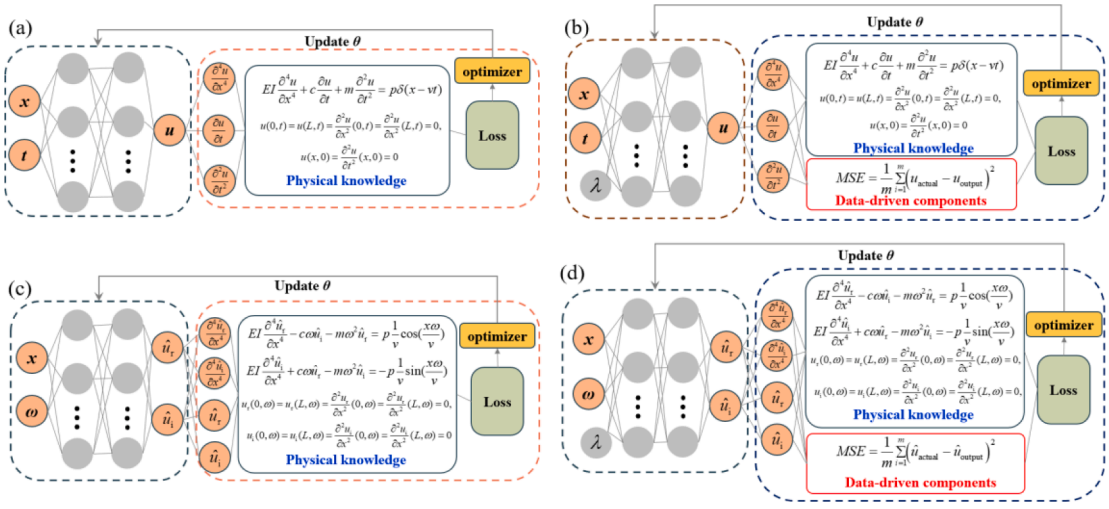

Fig. 1. The framework of PINN models for (a) solving forward problems and (b) solving inverse problems, and the framework of proposed FD-PINN models for (c) solving forward problems and (d) solving inverse problems. In solving the forward problem, the spatial and temporal or frequency variables x and t or ω serve as inputs to the neural network, while the corresponding displacements are its outputs. The PDE governing the problem is integrated into the model and used for training. In solving the inverse problem, the parameters to be identified are treated as training parameters, and actual data is incorporated into the training process. This enables the model to identify unknown parameters while simulating the structural dynamic response.

$$EI\frac{\partial^4 \widehat{u}_{\mathrm{r}}(x,\omega)}{\partial x^4} - c\omega\widehat{u}_{\mathrm{i}}(x,\omega) - m\omega^2\widehat{u}_{\mathrm{r}}(x,\omega) = p\frac{1}{v}\cos\left(\frac{x\omega}{v}\right), \tag{15}$$

$$EI\frac{\partial^4 \widehat{u}_{\mathrm{i}}(x,\omega)}{\partial x^4} + c\omega\widehat{u}_{\mathrm{r}}(x,\omega) - m\omega^2\widehat{u}_{\mathrm{i}}(x,\omega) = -p\frac{1}{v}\sin\left(\frac{x\omega}{v}\right). \tag{16}$$

For the above governing equations in the frequency domain, a PINN can be developed for forward solving the response of simply supported beams under moving load, as shown in Fig. 1 (c). Also, the boundary conditions in Eq. (2) need to be transformed to the frequency domain and considered in the loss function of the neural network, which is as follows:

$$\widehat{u}(0,\omega) = \widehat{u}(L,\omega) = \frac{\partial^2\widehat{u}}{\partial x^2}(0,\omega) = \frac{\partial^2\widehat{u}}{\partial x^2}(L,\omega) = 0. \tag{17}$$

It should be noted that it is usually difficult to consider the special initial conditions in the frequency domain, and the solution results in the frequency domain are consistent with those for stationary initial conditions. Considering that the response of the beams under the moving load usually takes the stationary state as the initial condition, which response can be considered as a periodic function on the time scale. Therefore, it is feasible to use the FD-PINN for solving the structural dynamic issue in this study. The schematic of the computational domain and sampling points used in model training for PINN and FD-PINN is shown in Fig. 2, it can be noticed that different random sampling strategies are used in FD-PINN since the results of the equations at different frequencies are decoupled.

In addition, since the network uses frequencies as inputs, which means that the frequency range of the computational domain needs to be set appropriately before the computation. It should be noted that the range of frequencies used in the actual calculation cannot be infinite. Therefore, the original problem can be approximated by selecting the range of frequencies based on its major frequency components. The principles for selecting calculation frequency ranges in spectral numerical methods [67] can be used as references for FD-PINN. Considering that the dynamic response of simply supported beams under moving loads is mainly composed of the first-order mode [57], the frequency input range of the neural network in this paper is expected to contain the first-order natural frequency of the structure. For other issues, the computational frequency range should also be set by referencing the frequency components of the load. In addition, in some engineering applications, such as simulating train induced vibrations, the frequency range can be determined based on specific requirements in engineering.

In addition, given that the Dirac functions in the control equations are not feasible in numerical computations, the Gaussian function is employed in this study as an approximation, the details are described in Appendix A.

After calculating the response spectrum of the beam in the frequency domain using FD-PINN, the inverse Fourier transform can be used to obtain the solution of the original equations in the time domain, which is shown below:

$$u(x,t) = \frac{1}{2\pi}\int_{-\infty}^{+\infty}\widehat{u}(x,\omega)e^{\mathrm{i}\omega t}d\omega. \tag{18}$$

Similarly, for solving inverse problems such as parameter identification using FD-PINN, both the PDE and the measurement data need to be transformed into the frequency domain using the Fourier transform, including their real and imaginary parts. Specifically, the discrete Fourier transform (DFT) [68] can be used to transform the measurement data into the frequency domain as follows:

$$\widehat{u}(k) = \sum_{n=0}^{N-1} u(n)\cdot e^{-\mathrm{i}\frac{2\pi}{N}kn}, \tag{19}$$

where $\widehat{u}(k)$ is the k-th frequency component of the frequency domain signal; $u(n)$ is the n-th sample of the time domain signal; N is the total number of samples in the signal; $e^{-\mathrm{i}\frac{2\pi}{N}kn}$ is the Fourier basis function, used to project the time domain signal into the frequency domain.

The procedure for solving simply supported beams under moving loads using the FD-PINN method is summarized in Fig. 3.

3. Forward simulation of structural dynamics

In this section, the structural dynamics under various moving load conditions are presented, and traditional PINN, gPINN, SA-PINN, and the proposed FD-PINN are implemented to address these problems. Specifically, Section 3.1 describes the details of the structural dynamics cases, and Section 3.2 introduces the implementation details of the models. Section 3.3 presents the calculation results of the models.

3.1. Calculation setup

To evaluate the performance of the FD-PINN method in forward solving the aforementioned problems, three cases are presented in this section. Additionally, according to the basic theory of dynamic response of simply supported beams under moving loads presented in Section 2.1, the calculation results of the analytical model based on the modal superposition method are utilized as a reference, and the forward simulation performance of each model on its dynamic response is investigated. The parameters used in various cases are shown in Table 1. In addition, the models were also built on another set of parameters, the details of which and the results of the model calculations are shown in

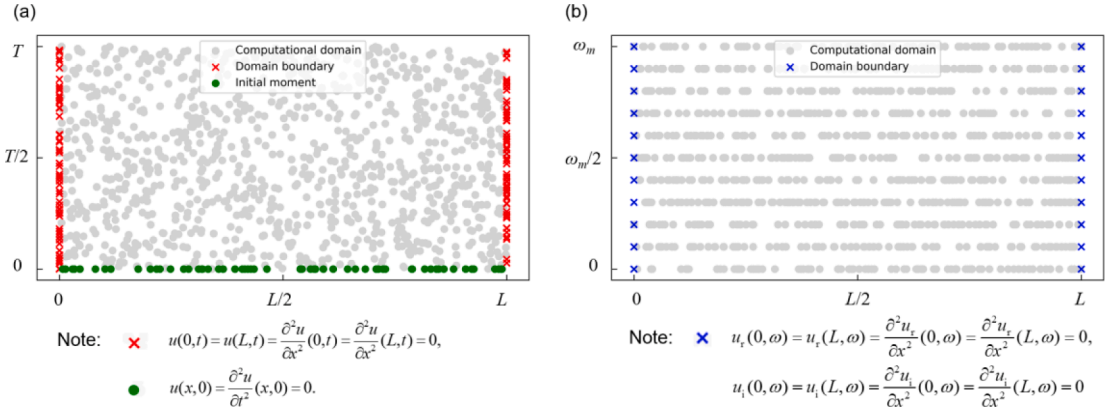

Fig. 2. Schematic of the computational domain and sampling points used in model training for (a) PINN and (b) FD-PINN. The training points are randomly sampled from this time-space domain, and in order for the solution of the model to satisfy the initial and boundary conditions in the PDE, additional training points need to be sampled at the corresponding times and boundaries.

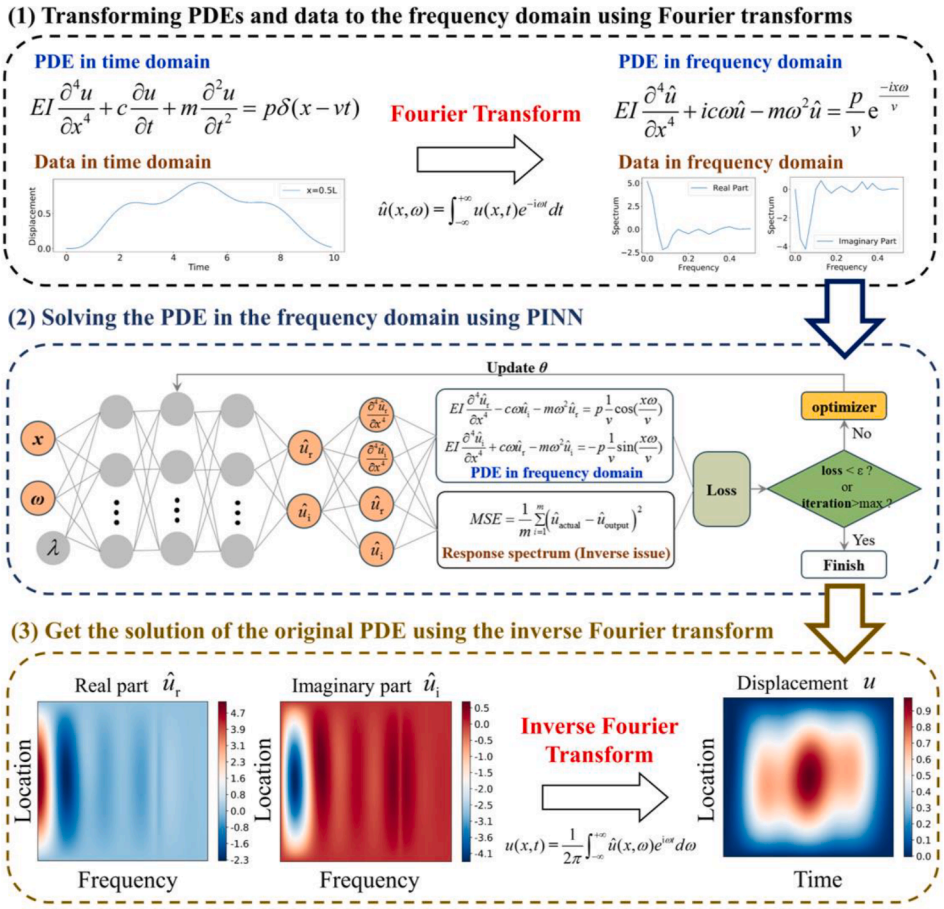

Fig. 3. Solution procedure for simply supported beams under moving loads using the FD-PINN method. Specifically, the equations and data need to be represented in the frequency domain before being fed into the neural network, and then the PINN is used to solve for the spectrum of the dynamic response, after which the inverse Fourier transform is utilized to obtain the solution of the original PDE.

Table 1
Mechanical parameters used in the cases.

	v (m/s)	L (m)	EI (N·m^2)	m (kg/m)	ξ	ω_1 (rad/s)	p (kN)
Case 1	50	20	2.4×10^9	3000	0.025	22.069	12
Case 2	20	20	2.4×10^9	3000	0.025	22.069	12
Case 3	15	20	2.4×10^9	3000	0.025	22.069	12

Appendix B.

3.2. Model implementation

Following the methodology presented in Section 2, neural network models including FD-PINN, PINN, gPINN, SA-PINN are developed respectively to solve the dynamic response of simply supported beams mentioned above. Since the forced vibration response of the beam is the main concern in the above problem, the time domain used for the calculations is [0, L/v], which is the period of the beam subjected to the moving load. Whereas, in the neural network developed using the FD-PINN method, the calculations are carried out in the spatial-frequency domain, and the frequency domain used for the calculations is considered as [0, 5] Hz, which envelopes main frequency components of the dynamic response of the structure [57]. The parameter σ in the Gaussian function used to approximate the Dirac function in moving loads is set to 0.1.

Neural networks with the same structure were developed respectively. Specifically, the built neural network contains three hidden layers, each containing 60 hidden cells, and the hyperbolic tangent function is used as the activation function in the network, which is considered to be a suitable activation function for PINN computation [69].

For model training, the Glorot uniform method [70] is used to initialize networks, 20,000 collection points were randomly sampled over the computational domain to calculate the model losses and for updating the model weights, the Limited-memory Broyden--Fletcher-Goldfarb-Shanno (L-BFGS) optimiser [71] was utilised to train the model, the number of iterations for model training was chosen to be 400,000. Additionally, the training point resampling technique has been adopted [72], allowing the model to randomly resample the training points on the computational domain after every 100 training iterations, which helps the model to avoid overfitting to a specific set of training points, thereby promoting a more generalized learning of the solution across the entire domain [73]. The coefficients of each sub-term of the loss function were set to the reciprocal of their initial values, ensuring that the initial values of each sub-term within the loss function are approximately equal. Furthermore, the output transform technique was utilized to scale the network output to more sensitive values of the activation function, thereby improving the performance of the models [74].

In recent years, numerous platforms for PINN computation have been proposed, greatly facilitating the implementation of PINN, such as Neurodiffeq [75], NVIDIA SimNet [76], FastVPINNs [77]. DeepXDE [78] was utilized to implement the PINN in this paper. All numerical

calculations were performed on a standard workstation equipped with an NVIDIA Tesla V100 GPU (32 G). After each model was computed, the displacements of 101 × 101 = 10,201 points in the spatial- temporal domain were uniformly extracted for result comparison.

3.3. Result

Fig. 4 shows the variations of the loss function of the developed models with the number of iterations during the training process, and it can be found that the training loss of the models gradually decreases and almost no longer decreases as it stabilizes around 400,000 iterations, which suggests that the selected number of training iterations is reasonable.

The results of the displacement field calculated by the fully trained model on various cases are shown in Fig. 5 and Fig. 6, and the response results calculated by the PINN model and the FD-PINN model are shown in Fig. 7. The response of the beam under a moving load comprises two components: a low-frequency component, associated with the moving velocity, and a high-frequency component, related to the natural frequency of the beam.

In simulating the dynamic response of the beam using the PINN model, it often accurately captures the low-frequency components of the response but struggles to simulate the high-frequency components associated with the beam's natural frequency. Fig. 7 illustrates that while the overall trend of the dynamic response calculated by PINN aligns with the actual result, there remains a significant error in the simulation. This phenomenon is also observed in the simulation results of gPINN and SA-PINN. The underlying reason for this limitation lies in a common limitation of neural network simulation, where model weights are optimized to local optimal solutions during training but cannot achieve the global optimal solution [38,45]. As a result, when a neural network simulates a multi-frequency function, it might only be able to simulate the low-frequency components of the function while ignoring its high-frequency components, this phenomenon is also referred to as spectral bias in some research. Although gPINN adds additional constraints related to the derivatives of the PDE in the model training loss and SA-PINN uses adaptive loss coefficients, both still cannot avoid spectral bias in the simulation.

In contrast, the FD-PINN model proposed in this paper exhibits relatively low error compared to the analytical solution in nearly all cases, suggesting its feasibility in simulating the dynamic response of the beam under moving loads. This improvement arises from the transformation of the original PDE in the spatial-time domain to the spatial-frequency domain in the FD-PINN method. Consequently, the neural network is relieved from simulating the original complex function containing multi-frequency features in the solution, thereby significantly enhancing the accuracy of the simulation.

4. Parameter identification of structural dynamics

In this section, the parameter identification problem in structural dynamics is addressed, employing traditional PINN, gPINN, SA-PINN, and the proposed FD-PINN. Section 4.1 elaborates on the details of the parameter identification problem, while Section 4.2 introduces the implementation details of models. Subsequently, Section 4.3 presents the calculation results of the models.

4.1. Calculation setup

The inverse identification of structural parameters using the measured structural response under known moving loads is a classical inverse problem, and the performance of the FD-PINN models on this problem is investigated in this section. The calculation example for the inverse identification of structural parameters is presented. Specifically, the parameter of bending stiffness *EI* of the beam is unknown and needs to be identified. A sensor is positioned in the middle of the beam to access the beam's response under a moving load at this location. The parameters of the beams and loads in the cases are consistent with those in Section 3, as detailed in Table 1.

4.2. Model implementation

In the inverse problem solution of PINN, the difference between the measurement response and the model simulation result is considered in the loss function of the model, and the parameter to be identified is considered as a weight of the model, which is optimized and updated during the model training. The inverse identification results of the parameters and the solution of the model can be obtained after the training is completed. In addition, the parameters to be identified need to be initialized before the training of the model, and the initial value of *EI* is chosen as 5×10^9 N·m^2 in this study. The remaining details of the model implementation, such as the network size, model training method, chosen optimizer, computational platform, and other relevant information, are consistent with those outlined in Section 3.2 for the forward

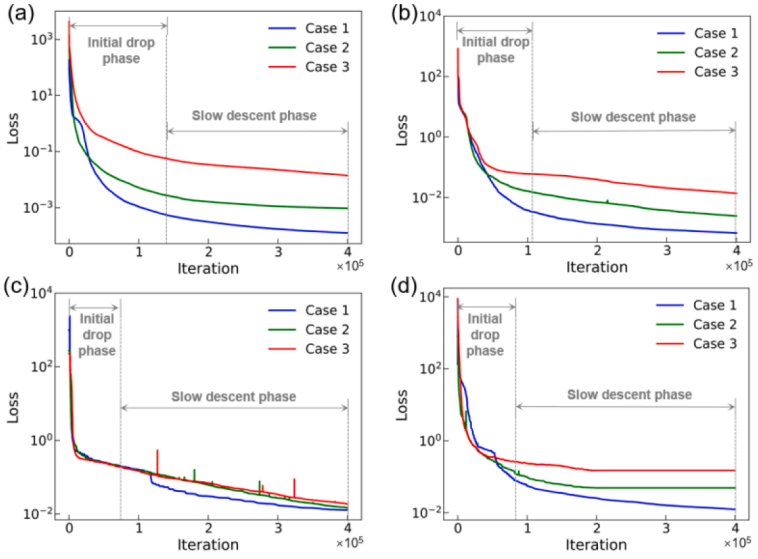

Fig. 4. Model training loss on various computational cases: (a) FD-PINN model, (b) PINN model, (c) gPINN model, (d) SA-PINN model. The loss functions of the models built based on all methods converged after being trained for 400,000 iterations.

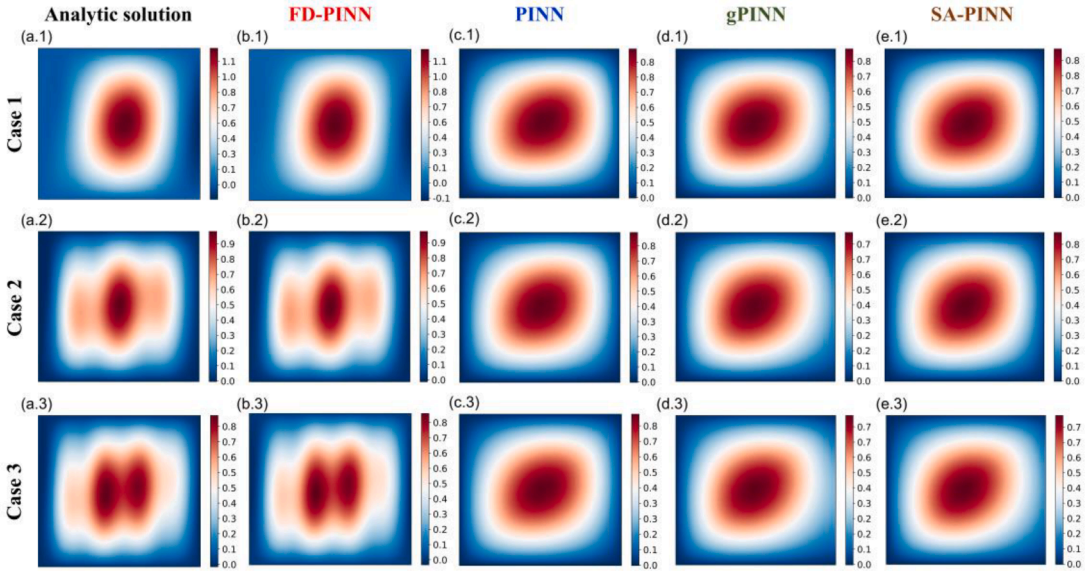

Fig. 5. The displacement field calculated by models across various cases (units: mm). In each displacement field, the horizontal coordinates represent time, the vertical coordinate represents positions on the beam, and the colors represent the amplitude of the structural dynamic response at different locations and moments.

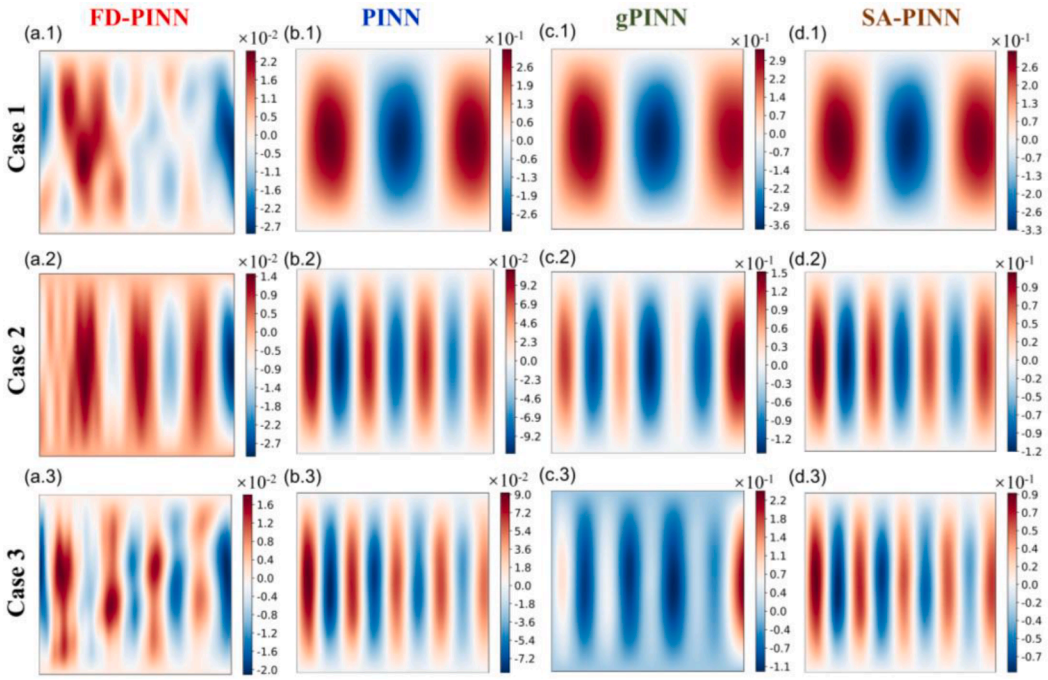

Fig. 6. The calculation errors of displacement fields by various models across different cases (units: mm). In each displacement field, the horizontal coordinates represent time, the vertical coordinate represents positions on the beam, and the colors depict the amplitude of the simulation error of structural dynamic response at different locations and moments.

simulation.

To compare the performance of the PINN model in forward and inverse solutions, the mean square error (MSE) between the model calculation results and the analytical solution was used to evaluate the accuracy of the model simulation, which is calculated as follows.

$$\mathrm{MSE} = \frac{1}{N}\sum_{i=1}^{N}(\widehat{y}_i - y_i)^2, \tag{20}$$

where y_i is the exact result of the ith sampling point in the calculation domain, $\widehat{y}_i$ is the value of the ith sampling point calculated by the models, and N is the total number of sampling points.

In addition, the magnitude of the displacement field on the computational domain in different cases is varied, the min-max normalization method was used before calculating the MSE to compare the model errors in the different cases, which is calculated as follows.

$$\widehat{y}_i^* = \frac{\widehat{y}_i - y_{\min}}{y_{\max} - y_{\min}}, \tag{21}$$

where $y_{\min}$ is the minimum value of the exact solution for all sampling points, $y_{\max}$ is the maximum value of the exact solution for all sampling points, $\widehat{y}_i$ is the output of the ith sampling point, $\widehat{y}_i^*$ is the normalized result of the model output for the ith sampling point.

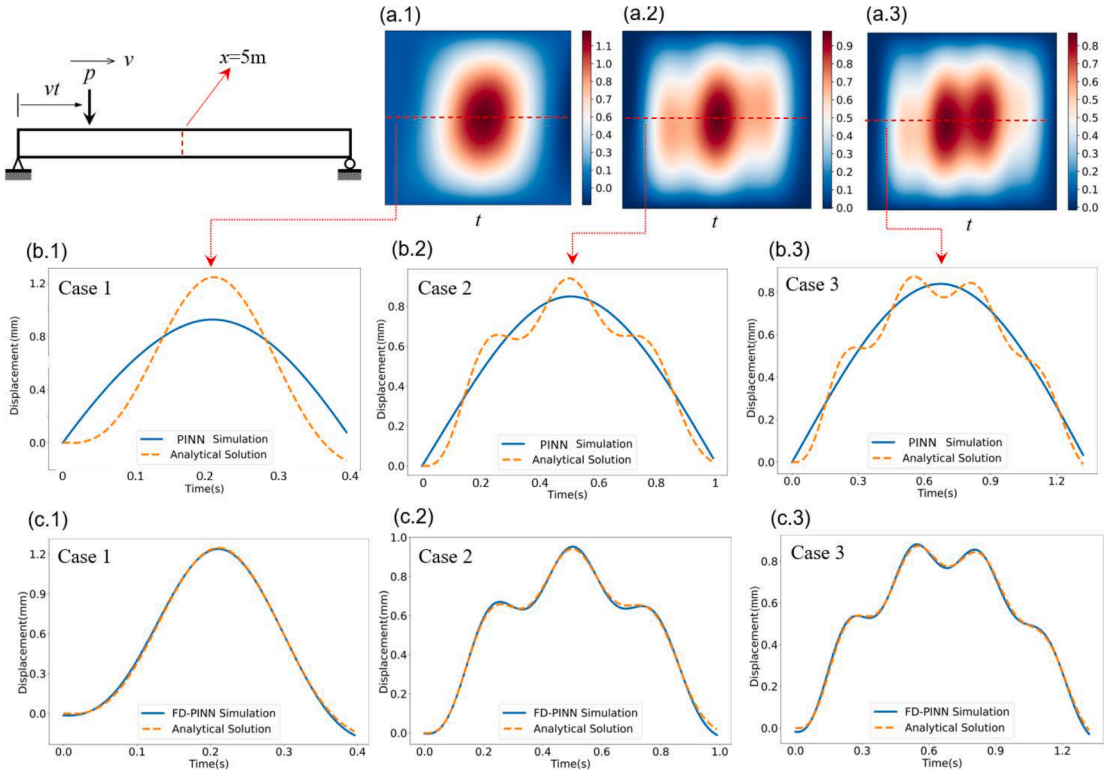

Fig. 7. Comparison of the dynamic response at the locations x=5 m of the beams with the (a) analytical solution computed by the (b) PINN model and (c) FD-PINN model in Cases. The blue line represents the simulation results obtained from the PINN and FD-PINN calculations, and the orange dashed line represents the actual analytical results.

Moreover, in order to quantitatively compare the accuracy of each model on parameter identification, the indicator of accuracy is defined as follows.

$$\text{Accuracy} = 1 - \frac{\left|EI_{\text{identified}} - EI_{\text{truth}}\right|}{EI_{\text{identified}}}, \tag{22}$$

where $EI_{\text{identified}}$ is the parameter result identified by various models, and EI_{truth} is the true parameter value.

4.3. Result

The results of parameter inverse identification by the models are shown in Fig. 8. It can be found that the two fully trained models can

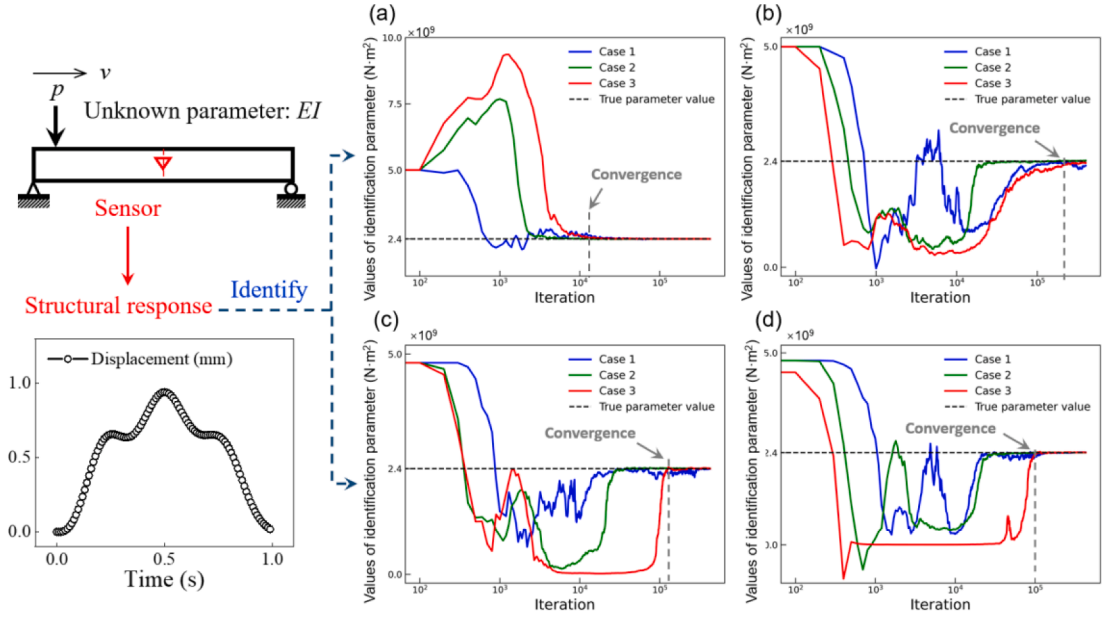

Fig. 8. Inverse identification results of parameters on various cases by (a) FD-PINN, (b) PINN, (c) gPINN, and (d)SA-PINN. The true parameter values are represented by black dashed lines, the variation of the parameter identification results with the number of iterations for the neural networks built based on the two methods is represented by solid lines.

almost identify the true parameter values in various cases, but there is a difference in the convergence speed and final accuracy of the identification results. Specifically, Table 2 demonstrates the identification results and accuracy of the four models on different iterations, and it can be seen that the PINN model could achieve relatively acceptable identification results on about 1×10^4 iterations, and the final identification accuracy of the model after training 4×10^5 iterations is about 95 % in various cases. The performance of gPINN and SA-PINN is slightly better than that of the traditional PINN, especially after 4×10^5 iterations of training, the parameter identification results of both of them are almost 100 %, but the convergence speed of their identification results are relatively poor, and neither of them achieves effective parameter identification when the model has been trained for 1×10^4 iterations. The FD-PINN model proposed in this paper achieved significantly faster convergence in parameter identification, and it converged to a relatively great identification result at about 1×10^4 iterations, and the identification accuracy of the model is more than 99 % on both 1×10^5 iterations and 4×10^5 iterations of training.

Overall, the above calculation results demonstrate the feasibility of the PINN methods for structural dynamic parameter identification. Moreover, the FD-PINN method proposed in this paper achieves higher accuracy and faster convergence than the traditional PINN method in structural dynamic parameter identification.

The displacement field calculated by the models in parameter inverse identification is shown in Fig. 9, and the MSE of the model for forward simulation and inverse simulation are shown in Table 3. It can be seen that the performance of almost all models in the inverse simulation is superior to their performance in the forward simulation. Specifically, on Cases 1 and 2, all the PINN, gPINN, and SA-PINN were able to achieve simulation of the natural frequencies of the structure at higher frequencies in the inverse simulation, which is significantly better than the original results on the forward simulation. This could be attributed to the fact that in the inverse simulation, the model is provided with the dynamic response of the beam at certain positions, thereby reducing the complexity of the simulation and facilitating the attainment of the global optimal solution rather than settling for a local optimal solution. These results suggest that the addition of measured data to the training of PINN is able to improve the ability of the model to deal with the spectral bias problem. However, in Case 3, the three models still struggle to simulate the high-frequency component of the dynamic response, which is dependent on the natural frequency, despite minor errors in parameter identification. This may be due to the fact that the solution of the equations in that case is more complicated, or the measurement data provided is not the most beneficial information for the model simulation.

Additionally, it is noted that among the cases, the PINN simulation error is highest for Case 1 and lowest for Case 3. This discrepancy arises from the fact that the load is moving at its maximum speed in Case 1, leading to the highest proportion of the high-frequency response component of the beam, whereas it is the smallest in Case 3. Given that the high-frequency response component is challenging for PINN to simulate, this results in a notable disparity in the simulation error of PINN for each case.

In contrast, the error of the FD-PINN model in the inverse simulation is lower than that of the PINN model, and is also marginally lower than that of the FD-PINN model in the forward simulation. This highlights the greater potential of the PINN method in inverse analysis compared to forward analysis.

5. Conclusions

In this paper, a PINN framework for both forward simulation and inverse parameter identification of structural dynamics is developed. Additionally, the FD-PINN method is proposed to address the challenge of spectral bias in neural networks when simulating multi-frequency functions. Specifically, this method involves transforming the original PDE from the time domain to the frequency domain using the Fourier transform, thereby reducing the simulation complexity for the neural network and enhancing its accuracy. Furthermore, typical structural dynamics cases are presented, focusing on the dynamic responses of simply supported beams under moving loads. The calculations conducted with the proposed FD-PINN method are compared with those using the traditional PINN method across these cases.

The calculation results indicate that the traditional PINN method was only able to simulate the low-frequency components of the structural dynamic response, failing to capture the high-frequency components associated with the natural frequencies of the structure. Consequently, this resulted in lower simulation accuracy. In contrast, the proposed FD-PINN method effectively overcomes this challenge, achieving an accurate simulation of the structural dynamic response. Specifically, the proposed FD-PINN can reduce the mean-square error of the simulation to below about 7×10^{-5} in various cases, while that of the traditional PINN is about 1.5×10^{-3} or more. In addition, for the inverse identification of structural parameters, both the PINN and FD-PINN methods can achieve better identification results, while the proposed FD-PINN can achieve higher convergence speed and identification accuracy. For example, after the same training of 1×10^4 iterations, the proposed FD-PINN can achieve a parameter identification accuracy of more than 94 % across all cases, while the accuracy of the PINN is below 68 %. In conclusion, the results demonstrate the feasibility and the superiority of the proposed FD-PINN method for forward simulation and inverse parameter identification of structural dynamics.

Furthermore, it's important to highlight that the FD-PINN proposed in this paper alleviates the complexity of solving the original PDE through integral transformation, thereby addressing the spectral bias in neural network simulation. However, the mechanism underlying

Table 2
Inverse identification results of parameters by models on various iterations.

Model	Training Iteration ($\times 10^4$)	Case 1		Case 2		Case 3	
		Identified result (10^9 N·m^2)	Accuracy	Identified result (10^9 N·m^2)	Accuracy	Identified result (10^9 N·m^2)	Accuracy
FD-PINN	1	2.409	99.6 %	2.500	95.8 %	2.534	94.4 %
	10	2.400	100.0 %	2.405	100.2 %	2.405	99.8 %
	40	2.400	100.0 %	2.400	100.0 %	2.400	100.0 %
PINN	1	1.632	68.0 %	0.557	23.2 %	0.328	13.7 %
	10	2.323	96.8 %	2.386	99.4 %	2.213	92.2 %
	40	2.299	95.8 %	2.414	99.4 %	2.362	98.4 %
gPINN	1	1.301	54.20 %	0.300	12.52 %	0.027	1.12 %
	10	2.280	95.00 %	2.410	99.60 %	1.306	54.40 %
	40	2.386	99.40 %	2.405	99.80 %	2.410	99.60 %
SA-PINN	1	0.285	11.88 %	0.401	16.72 %	0.002	0.09 %
	10	2.290	95.40 %	2.390	99.60 %	2.381	99.20 %
	40	2.405	99.80 %	2.400	100.00 %	2.410	99.60 %

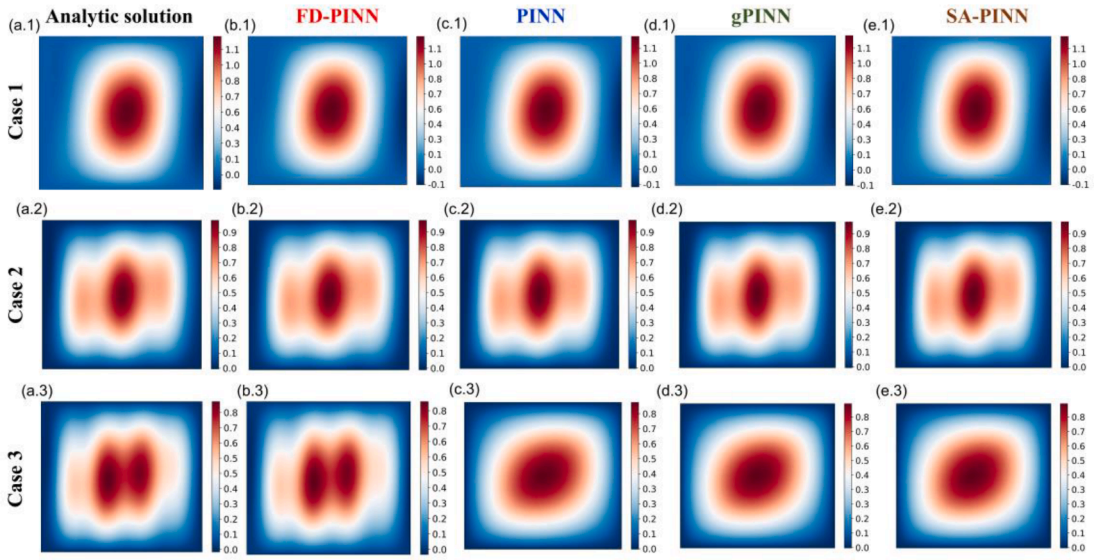

Fig. 9. Displacement fields calculated by the model in parameter inverse identification in various cases (units: mm). In each displacement field, the horizontal coordinates represent time, the vertical coordinate represents positions on the beam, and the colors depict the amplitude of the simulation error of structural dynamic response at different locations and moments.

Table 3
The MSE results of the model in forward simulation and inverse simulation on various cases.

Model	Case 1		Case 2		Case 3	
	Forward	Inverse	Forward	Inverse	Forward	Inverse
FD-PINN	4.72E-05	4.69E-05	7.15E-05	6.47E-05	7.01E-05	7.01E-05
PINN	1.39E-02	1.10E-04	2.43E-03	1.00E-04	1.56E-03	1.56E-03
gPINN	1.83E-02	1.10E-04	3.99 E-03	1.02E-04	3.50E-03	1.70E-03
SA-PINN	1.41E-02	1.09 E-04	2.53E-03	1.02 E-04	1.61E-03	1.61E-03

spectral bias in neural networks, as well as more comprehensive solution methods, warrant further investigation in future research endeavors. Moreover, while incorporating physical constraints into the model via PINN enhances the physical system simulations, it inevitably introduces additional complexity. Future research is needed to address this challenge, focusing on strategies to balance the integration of physical constraints with the optimization of simulation efficiency, ultimately leading to more accurate and computationally efficient simulations.

CRediT authorship contribution statement

Ruihua Liang: Writing – review & editing, Writing – original draft, Methodology, Investigation, Data curation. **Weifeng Liu:** Writing – review & editing, Supervision, Resources. **Yuguang Fu:** Writing – review & editing, Supervision, Resources. **Meng Ma:** Writing – review & editing, Resources.

Declaration of competing interest

The authors declare that they have no known competing financial interests or personal relationships that could have appeared to influence the work reported in this paper.

Data availability

The source codes to reproduce the results in this study are available on GitHub at https://github.com/railleon/FD-PINN_dynamics upon final publication.

Acknowledgements

This research/project was supported by Beijing Natural Science Foundation (Grant No. L221021), the National Natural Science Foundation of China (Grant No. 52178404), the National Research Foundation, Singapore under its AI Singapore Programme (AISG Award No: AISG2-TC-2021-001), and The Ministry of Education Tier 1 Grants, Singapore (No. RG121/21 and No. RS04/21).

Appendix A. Numerical approximation of the Dirac function

The Gaussian function is employed in this study as an approximation of Dirac functions, the relationship between these two functions can be expressed as follows [79,80],

$$\delta(x) = \lim_{a\to\infty} \frac{1}{\sqrt{2\pi\sigma^2}} e^{-\frac{x^2}{2\sigma^2}}. \tag{23}$$

Therefore, $\frac{1}{\sqrt{2\pi\sigma^2}} e^{-\frac{x^2}{2\sigma^2}}$ is used in this research to approximate the Dirac function, where the parameter σ is assigned a small value.

Appendix B. Supplementary calculations

The parameters of the structure and loads used in the supplementary calculations were selected with reference to the research [81], which is shown in Table B1. The proposed FD-PINN and the traditional PINN were established to compute the dynamic response of the structure. The implementation details and parameters of the models can be found in Section 3.2, the calculated displacement field of the models is shown in Fig. B1. It can be seen that the proposed FD-PINN still achieves significantly more accurate simulations than the PINN, especially on the high-frequency component of the response, which is similar to the results shown in Section 3, which further proves the superiority of the proposed FD-PINN.

Table B1
Mechanical parameters used in the cases.

	v (m/s)	L (m)	EI (N·m^2)	m (kg/m)	ξ	p (kN)
Case B1	30	20	29.4×10^9	34,088	0.025	215.6
Case B2	20	20	29.4×10^9	34,088	0.025	215.6
Case B3	10	20	29.4×10^9	34,088	0.025	215.6

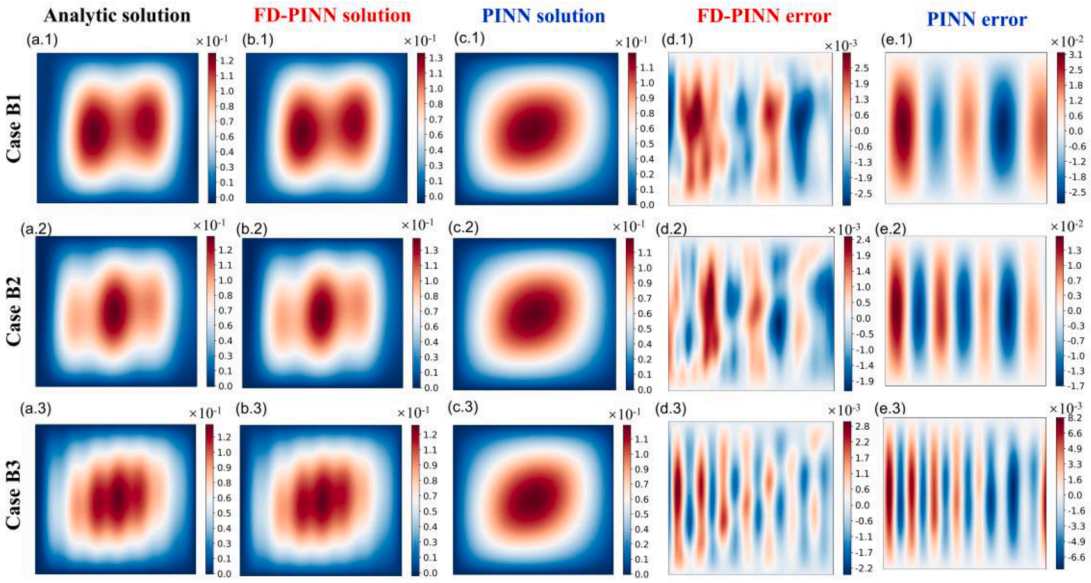

Fig. B1. The displacement field calculated by models across various cases and the corresponding calculation error (units: mm). In each displacement field, the horizontal coordinates represent time, the vertical coordinate represents positions on the beam, and the colors represent the amplitude of the structural dynamic response at different locations and moments.

References

[1] An Y, Chatzi E, Sim S-H, Laflamme S, Blachowski B, Ou J. Recent progress and future trends on damage identification methods for bridge structures. Struct Control Health Monit 2019;26:e2416.

[2] Liu W, Tong L, Li H, Wang Z, Sun Y, Gu W. Multi-parameter intelligent inverse analysis of a deep excavation considering path-dependent behavior of soils. Comput Geotech 2024;174:106597.

[3] Dessena G, Civera M, Zanotti Fragonara L, Ignatyev DI, Whidborne JF. A loewner-based system identification and structural health monitoring approach for mechanical systems, struct. Control Health Monit 2023;2023:1–22. https://doi.org/10.1155/2023/1891062.

[4] Jarfi H, Eskandari M, KA KA. Development of governing partial differential equations of reinforcing thin films. Int J Mech Sci 2024;276:109407.

[5] Xu YF, Huang GL. Modal sensitivity analysis of acoustic metamaterials for structural damage detection. Int J Mech Sci 2023;259:108571.

[6] Ding W, Semperlotti F. A multimesh finite element method for integral nonlocal elasticity using mesh-decoupling technique. Int J Mech Sci 2024;275:109260.

[7] Yang X-D, Zhang W, Chen L-Q, Yao M-H. Dynamical analysis of axially moving plate by finite difference method. Nonlinear Dyn 2012;67:997–1006. https://doi.org/10.1007/s11071-011-0042-2.

[8] Jin D, Guo Y, Li X, Yuan D, Shu J, Chen J, Li F. Modeling of reinforced-concrete cutting with shield rippers using FEM-DEM-coupling method. Int J Mech Sci 2024;282:109619.

[9] Ji W, Ma H, Liu F, Sun W, Wang D. Dynamic analysis of cracked pipe elbows: Numerical and experimental studies. Int J Mech Sci 2024;281:109580.

[10] Pfeil S, Gravenkamp H, Duvigneau F, Woschke E. Semi-analytical solution of the Reynolds equation considering cavitation. Int J Mech Sci 2023;247:108164.

[11] Zhao Y, Zhou Z, Bi J, Wang C. Simulation of brittle fractures using energy-bond-based smoothed particle hydrodynamics. Int J Mech Sci 2023;248:108236.

[12] Fan H, Li L, Chen G, Liu H, Ji X, Jiang X, Zhou S. An improved 3D DDA method considering the unloading effect of tunnel excavation and its application. Comput Geotech 2023;154:105178. https://doi.org/10.1016/j.compgeo.2022.105178.

[13] Peng H, Yan J, Yu Y, Luo Y. Time series estimation based on deep learning for structural dynamic nonlinear prediction, in: structures. Elsevier; 2021. p. 1016–31. https://www.sciencedirect.com/science/article/pii/S2352012420306901. accessed March 31, 2024.

[14] Liang R, Liu W, Ma M, Liu W. An efficient model for predicting the train-induced ground-borne vibration and uncertainty quantification based on Bayesian neural network. J Sound Vib 2021;495:115908.

[15] Tsialiamanis G, Dervilis N, Wagg DJ, Worden K. Towards a population-informed approach to the definition of data-driven models for structural dynamics. Mech Syst Signal Process 2023;200:110581.

[16] Liang R, Liu W, Li C, Li W, Wu Z. A novel efficient probabilistic prediction approach for train-induced ground vibrations based on transfer learning. J Vib Control 2023:10775463221148792.

[17] Bao Y, Tang Z, Li H, Zhang Y. Computer vision and deep learning–based data anomaly detection method for structural health monitoring. Struct Health Monit 2019;18:401–21.

[18] Ye XW, Jin T, Yun CB. A review on deep learning-based structural health monitoring of civil infrastructures. Smart Struct Syst 2019;24:567–85.

[19] Li C, Liu W, Liang R. Identification of vertical wheel-rail contact force based on an analytical model and measurement and its application in predicting ground-borne vibration. Measurement 2021;186:110182.

[20] Yang H, Jiang J, Chen G, Zhao J. Dynamic load identification based on deep convolution neural network. Mech Syst Signal Process 2023;185:109757.

[21] Liang R, Liu W, Li W, Wu Z. A traffic noise source identification method for buildings adjacent to multiple transport infrastructures based on deep learning. Build Environ 2022;211:108764.

[22] Liu W, Liang R, Zhang H, Wu Z, Jiang B. Deep learning based identification and uncertainty analysis of metro train induced ground-borne vibration. Mech Syst Signal Process. 2023;189:110062.
[23] Park S, Marimuthu KP, Han G, Lee H. Deep learning based nanoindentation method for evaluating mechanical properties of polymers. Int J Mech Sci 2023;246:108162.
[24] Liang R, Liu W, Kaewunruen S, Zhang H, Wu Z. Classification of external vibration sources through data-driven models using hybrid CNNs and LSTMs, struct. Control Health Monit 2023;2023:1–18. https://doi.org/10.1155/2023/1900447.
[25] Zhang Z, Li H, Hu Y, Liu Y, Li Y, Li B. Few-sample information-enhanced inverse design framework for customizing transmission-modulated elastic metasurfaces. Int J Mech Sci 2024;279:109507.
[26] Xiong Z, Yang P, Zhao P. Physics-driven neural networks for nonlinear micromechanics. Int J Mech Sci 2024;273:109214.
[27] Shang L, Zhao Y, Zheng S, Wang J, Zhang T, Wang J. Quantification of gradient energy coefficients using physics-informed neural networks. Int J Mech Sci 2024;273:109210. https://doi.org/10.1016/j.ijmecsci.2024.109210.
[28] Batuwatta-Gamage CP, Rathnayaka CM, Karunasena HCP, Jeong H, Karim MA, Gu YT. A physics-informed neural network framework to investigate nonlinear and heterogenous shrinkage of drying plant cells. Int J Mech Sci 2024;275:109267. https://doi.org/10.1016/j.ijmecsci.2024.109267.
[29] Liu C-X, Wang X, Liu W, Yang Y-F, Yu G-L, Liu Z. A physics-informed neural network for Kresling origami structures. Int J Mech Sci 2024;269:109080. https://doi.org/10.1016/j.ijmecsci.2024.109080.
[30] Zhang B, Wu G, Gu Y, Wang X, Wang F. Multi-domain physics-informed neural network for solving forward and inverse problems of steady-state heat conduction in multilayer media. Phys Fluids 2022;34.
[31] Cai S, Wang Z, Wang S, Perdikaris P, Karniadakis GE. Physics-informed neural networks for heat transfer problems. J Heat Transf 2021;143:060801.
[32] Eivazi H, Tahani M, Schlatter P, Vinuesa R. Physics-informed neural networks for solving Reynolds-averaged Navier-Stokes equations. Phys Fluids 2022;34. https://doi.org/10.1063/5.0095270.
[33] Ranade R, Hill C, Pathak J. DiscretizationNet: A machine-learning based solver for Navier–Stokes equations using finite volume discretization. Comput Methods Appl Mech Eng 2021;378:113722. https://doi.org/10.1016/j.cma.2021.113722.
[34] Liang R, Liu W, Xu L, Qu X, Kaewunruen S. Solving elastodynamics via physics-informed neural network frequency domain method. Int J Mech Sci 2023:108575.
[35] Rao C, Sun H, Liu Y. Physics-informed deep learning for computational elastodynamics without labeled data. J Eng Mech 2021;147:04021043.
[36] Bai J, Rabczuk T, Gupta A, Alzubaidi L, Gu Y. A physics-informed neural network technique based on a modified loss function for computational 2D and 3D solid mechanics. Comput Mech 2023;71:543–62. https://doi.org/10.1007/s00466-022-02252-0.
[37] Zheng B, Li T, Qi H, Gao L, Liu X, Yuan L. Physics-informed machine learning model for computational fracture of quasi-brittle materials without labelled data. Int J Mech Sci 2022;223:107282.
[38] Tancik M, Srinivasan P, Mildenhall B, Fridovich-Keil S, Raghavan N, Singhal U, Ramamoorthi R, Barron J, Ng R. Fourier features let networks learn high frequency functions in low dimensional domains. Adv Neural Inf Process Syst 2020;33:7537–47.
[39] Fridovich-Keil S, Gontijo Lopes R, Roelofs R. Spectral bias in practice: the role of function frequency in generalization. Adv Neural Inf Process Syst 2022;35:7368–82.
[40] Yang YB, Chen L, Wang ZL, Liu ZY, Liu D-H, Yao H, Zheng Y. Cancellation of resonance for elastically supported beams subjected to successive moving loads: Optimal design condition for bridges. Eng Struct 2024;307:117950. https://doi.org/10.1016/j.engstruct.2024.117950.
[41] Xu L, Ma M, Cao R, Tan X, Liang R. Effect of longitudinally varying characteristics of soil on metro train-induced ground vibrations based on wave propagation analysis. Soil Dyn Earthq Eng 2022;152:107020.
[42] Hester D, Brownjohn J, Huseynov F, Obrien E, Gonzalez A, Casero M. Identifying damage in a bridge by analysing rotation response to a moving load. Struct Infrastruct Eng 2020;16:1050–65. https://doi.org/10.1080/15732479.2019.1680710.
[43] Ma M, Xu L, Liu W, Tan X. Semi-analytical solution of a coupled tunnel-soil periodic model with a track slab under a moving train load. Appl Math Model 2024;128:588–608.
[44] Shao D, Li B, Cao Y, Tao Y, Sun N, Shi Y. Dynamic responses of composite plate-shell coupled structures under moving excitations. Int J Mech Sci 2024;265:108884.
[45] Wang S, Wang H, Perdikaris P. On the eigenvector bias of Fourier feature networks: From regression to solving multi-scale PDEs with physics-informed neural networks. Comput Methods Appl Mech Eng 2021;384:113938.
[46] Wang S, Yu X, Perdikaris P. When and why PINNs fail to train: a neural tangent kernel perspective. J Comput Phys 2022;449:110768.
[47] Chai X, Cao W, Li J, Long H, Sun X. Overcoming the spectral bias problem of physics-informed neural networks in solving the frequency-domain acoustic wave equation. IEEE Trans Geosci Remote Sens 2024. https://doi.org/10.1109/TGRS.2024.3440471. 1–1.
[48] Zhao Z, Shi D. Adaptive control of spectral bias in untrained neural network priors for inverse problems. Expert Syst Appl 2024;255:124516. https://doi.org/10.1016/j.eswa.2024.124516.
[49] Ding W, He Q, Tong H, Wang Q, Wang P. Solving coupled differential equation groups using PINO-CDE. Mech Syst Signal Process. 2024;208:111014.
[50] Waheed UB. Kronecker Neural Networks Overcome Spectral Bias for PINN-Based Wavefield Computation. IEEE Geosci Remote Sens Lett 2022;19:1–5. https://doi.org/10.1109/LGRS.2022.3209901.
[51] Zhang R, Liu Y, Sun H. Physics-guided convolutional neural network (PhyCNN) for data-driven seismic response modeling. Eng Struct 2020;215:110704. https://doi.org/10.1016/j.engstruct.2020.110704.
[52] Nuruddeen RI, Muhammad L, Nass AM, Sulaiman TA. A review of the integral transforms-based decomposition methods and their applications in solving nonlinear PDEs. Palest J Math 2018;7:262–80.
[53] Duhamel P, Vetterli M. Fast Fourier transforms: a tutorial review and a state of the art. Signal Process 1990;19:259–99.
[54] Helms H. Fast Fourier transform method of computing difference equations and simulating filters. IEEE Trans Audio Electroacoustics 1967;15:85–90.
[55] Sallam O, Fürth M. On the use of Fourier Features-Physics Informed Neural Networks (FF-PINN) for forward and inverse fluid mechanics problems. Proc Inst Mech Eng Part M J Eng Marit Environ 2023;237:846–66. https://doi.org/10.1177/14750902231166424.
[56] Zhang T, Yan R, Zhang S, Yang D, Chen A. Application of Fourier feature physics-information neural network in model of pipeline conveying fluid. Thin-Walled Struct 2024;198:111693.
[57] Ouyang H. Moving-load dynamic problems: A tutorial (with a brief overview). Mech Syst Signal Process. 2011;25:2039–60. https://doi.org/10.1016/j.ymssp.2010.12.010.
[58] Wanxie Z, Xiangxiang Z. Method of separation of variables and Hamiltonian system. Numer Methods Partial Differ Equ 1993;9:63–75. https://doi.org/10.1002/num.1690090107.
[59] Xia H, Li HL, Guo WW, De Roeck G. Vibration Resonance and Cancellation of Simply Supported Bridges under Moving Train Loads. J Eng Mech 2014;140:04014015. https://doi.org/10.1061/(ASCE)EM.1943-7889.0000714.
[60] Raissi M. Deep hidden physics models: deep learning of nonlinear partial differential equations. J Mach Learn Res 2018;19:932–55.
[61] Raissi M, Perdikaris P, Karniadakis GE. Physics-informed neural networks: a deep learning framework for solving forward and inverse problems involving nonlinear partial differential equations. J Comput Phys 2019;378:686–707.
[62] Karniadakis GE, Kevrekidis IG, Lu L, Perdikaris P, Wang S, Yang L. Physics-informed machine learning. Nat Rev Phys 2021;3:422–40.
[63] Yu J, Lu L, Meng X, Karniadakis GE. Gradient-enhanced physics-informed neural networks for forward and inverse PDE problems. Comput Methods Appl Mech Eng 2022;393:114823.
[64] McClenny LD, Braga-Neto UM. Self-adaptive physics-informed neural networks. J Comput Phys 2023;474:111722. https://doi.org/10.1016/j.jcp.2022.111722.
[65] Ghayesh MH, Farokhi H, Zhang Y, Gholipour A. Nonlinear coupled moving-load excited dynamics of beam-mass structures. Arch Civ Mech Eng 2020;20:45. https://doi.org/10.1007/s43452-020-00040-2.
[66] Li J, Zhang H, Zhu D, Li C. A moving load amplitude spectrum for analyzing the resonance and vibration cancellation of simply supported bridges under moving loads. Eur J Mech-ASolids 2022;92:104428.
[67] Burns KJ, Vasil GM, Oishi JS, Lecoanet D, Brown BP. Dedalus: A flexible framework for numerical simulations with spectral methods. Phys Rev Res 2020;2:023068. https://doi.org/10.1103/PhysRevResearch.2.023068.
[68] Wang Z. Fast algorithms for the discrete W transform and for the discrete Fourier transform. IEEE Trans Acoust Speech Signal Process 1984;32:803–16.
[69] Wang S, Wang H, Perdikaris P. Learning the solution operator of parametric partial differential equations with physics-informed deeponets. Sci Adv 2021;7:eabi8605.
[70] Hanin B, Rolnick D. How to start training: The effect of initialization and architecture. Adv Neural Inf Process Syst 2018:31.
[71] Liu DC, Nocedal J. On the limited memory BFGS method for large scale optimization. Math Program 1989;45:503–28.
[72] Lu L, Pestourie R, Yao W, Wang Z, Verdugo F, Johnson SG. Physics-informed neural networks with hard constraints for inverse design. SIAM J Sci Comput 2021;43:B1105–32. https://doi.org/10.1137/21M1397908.
[73] Wu C, Zhu M, Tan Q, Kartha Y, Lu L. A comprehensive study of non-adaptive and residual-based adaptive sampling for physics-informed neural networks. Comput Methods Appl Mech Eng 2023;403:115671. https://doi.org/10.1016/j.cma.2022.115671.
[74] Wu C, Zhu M, Tan Q, Kartha Y, Lu L. A comprehensive study of non-adaptive and residual-based adaptive sampling for physics-informed neural networks. Comput Methods Appl Mech Eng 2023;403:115671.
[75] Chen F, Sondak D, Protopapas P, Mattheakis M, Liu S, Agarwal D, Di Giovanni M. Neurodiffeq: a python package for solving differential equations with neural networks. J Open Source Softw. 2020;5:1931.
[76] Hennigh O, Narasimhan S, Nabian MA, Subramaniam A, Tangsali K, Fang Z, Rietmann M, Byeon W, Choudhry S. NVIDIA SimNet™: An AI-accelerated multi-physics simulation framework. In: Int. Conf. Comput. Sci. Springer; 2021. p. 447–61.
[77] Anandh T, Ghose D, Ganesan S. FastVPINNs: An efficient tensor-based Python libraryfor solving partial differential equations using hp-Variational PhysicsInformed Neural Networks. J Open Source Softw 2024;9:6764. https://doi.org/10.21105/joss.06764.
[78] Lu L, Meng X, Mao Z, Karniadakis GE. DeepXDE: a deep learning library for solving differential equations. SIAM Rev 2021;63:208–28.
[79] Rivera MJ, Trujillo M, Romero-García V, López Molina JA, Berjano E. Numerical resolution of the hyperbolic heat equation using smoothed mathematical functions

instead of Heaviside and Dirac delta distributions. Int Commun Heat Mass Transf 2013;46:7–12. https://doi.org/10.1016/j.icheatmasstransfer.2013.05.017.
[80] Kärnä T, Deleersnijder E, De Brauwere A. Simple test cases for validating a finite element unstructured grid fecal bacteria transport model. Appl Math Model 2010; 34:3055–70. https://doi.org/10.1016/j.apm.2010.01.012.
[81] Kumar CPS. Vibration of simply supported beams under a single moving load_ a detailed study of cancellation phenomenon. Int J Mech Sci 2015.